Influence of ocean winds on the pelagic ecosystem in upwelling regions

Ryan R. Rykaczewski* and David M. Checkley, Jr.

Scripps Institution of Oceanography, University of California at San Diego, 9500 Gilman Drive, La Jolla, CA 92093-0218

Communicated by Russ E. Davis, University of California at San Diego, La Jolla, CA, December 17, 2007 (received for review March 1, 2007)

Upwelling of nutrient-rich, subsurface water sustains high productivity in the ocean's eastern boundary currents. These ecosystems support a rate of fish harvest nearly 100 times the global mean and account for >20% of the world's marine fish catch. Environmental variability is thought to be the major cause of the decadal-scale biomass fluctuations characteristic of fish populations in these regions, but the mechanisms relating atmospheric physics to fish production remain unexplained. Two atmospheric conditions induce different types of upwelling in these ecosystems: coastal, alongshore wind stress, resulting in rapid upwelling (with high vertical velocity, *w*); and wind-stress curl, resulting in slower upwelling (low *w*). We show that the level of wind-stress curl has increased and that production of Pacific sardine (*Sardinops sagax*) varies with wind-stress curl over the past six decades. The extent of isopycnal shoaling, nutricline depth, and chlorophyll concentration in the upper ocean also correlate positively with wind-stress curl. The size structure of plankton assemblages is related to the rate of wind-forced upwelling, and sardine feed efficiently on small plankters generated by slow upwelling. Upwelling rate is a fundamental determinant of the biological structure and production in coastal pelagic ecosystems, and future changes in the magnitude and spatial gradient of wind stress may have important and differing effects on these ecosystems. Understanding of the biological mechanisms relating fisheries production to environmental variability is essential for wise management of marine resources under a changing climate.

California Current | sardine | wind-stress curl

Worldwide, populations of sardine (*Sardinops* spp.) and anchovy (*Engraulis* spp.) have varied greatly over time, with plentiful catches of one often alternating with the other on the scale of decades (1). These fluctuations have severe consequences for the fishing, processing, and farming (e.g., poultry, swine, and tuna) industries that depend on the fisheries' landings for income and feed. Because these small pelagic fish often dominate the intermediate trophic level in upwelling ecosystems, their populations are crucial to the transfer of energy and biomass from lower to higher trophic levels (2). Despite >50 years of effort and focused oceanographic research, a mechanistic explanation for the large variability in Pacific sardine and northern anchovy populations in the California Current Ecosystem (CCE) remains obscure. Sediment records suggest that similar fluctuations occurred over the two millennia before the development of commercial fisheries (3). The changes in sardine and anchovy abundance during the past century are therefore thought to reflect natural environmental variability, exacerbated by fishing pressure (4).

Understanding of the mechanisms relating these population fluctuations to environmental variability has not progressed past empirical observations associating sardine and anchovy biomass with temperature (1, 5). Warm periods, favorable for sardine production, occurred most recently from the 1920s to the mid-1940s and from 1977 through the present. A cool period, favorable for anchovy, occurred from the mid-1940s through 1976 (1, 5). A shift to another cool period may have occurred after the 1997–1998 El Niño (6). Identification of warm and cold periods favorable for sardine and anchovy production has been important in describing multidecadal changes in pelagic fisheries, but this description does not provide the understanding necessary to predict how populations will vary under future conditions. Because cold periods are often associated with increased coastal upwelling and nutrient supply along the coast, the growth observed in the anchovy population during these phases is expected. However, the paradoxical growth of a massive sardine population (up to four times larger than the maximal anchovy population) during warm periods with weak coastal upwelling has puzzled fisheries oceanographers for decades (3, 7).

To investigate the relationship between climate and sardine growth in the CCE, we considered the two mechanisms by which winds supply surface waters with the nutrients required for biological production: "coastal upwelling" due to alongshore wind stress and "curl-driven upwelling" due to wind-stress curl. The importance of coastal upwelling to major fisheries production has long been recognized (8). In the traditional view of coastal upwelling ecosystems, biological productivity at all levels of the food web is attributed to persistent, alongshore, and equatorward wind stress in spring and summer. These winds force water away from the coastal boundary, a process known as Ekman transport. Nutrient-rich waters are drawn up into the euphotic zone to replace the surface waters that are forced offshore.

Curl-driven upwelling may also act as a significant source of nutrients in coastal pelagic ecosystems (9–13) and is responsible for the shoaling of isopycnals in the southern CCE during summer (14). Horizontal shear in the wind stress (wind-stress curl) over the open ocean results in a divergence of Ekman transport that is balanced by vertical transport. Although most areas of the subtropical ocean gyres are regions of anticyclonic wind-stress curl (downwelling), the eastern edge of the gyres (i.e., inshore of the wind-stress maximum) are zones of cyclonic wind-stress curl and upwelling (10, 12). Small areas of intense, positive wind-stress curl occur in the lee of major headlands leading to curl-driven upwelling with vertical velocity (*w*) comparable with the high *w* associated with coastal upwelling (13). However, the average *w* associated with curl-driven upwelling is slow, typically several times smaller than *w* associated with coastal upwelling in the CCE (15). The expansive regions of positive curl over the open ocean are the result of two characteristics of the eastern North Pacific: (*i*) the large-scale change in the orientation of the west coast of North America, from a coastline trending north to south poleward of 40° N latitude to a coastline oriented northwest to southeast in southern California; and (*ii*) the location of the maximal gradient between the

Author contributions: R.R.R. and D.M.C. designed research; R.R.R. performed research; R.R.R. and D.M.C. analyzed data; and R.R.R. and D.M.C. wrote the paper.

The authors declare no conflict of interest.

*To whom correspondence should be addressed. E-mail: rrykacze@ucsd.edu.

This article contains supporting information online at www.pnas.org/cgi/content/full/0711777105/DC1.

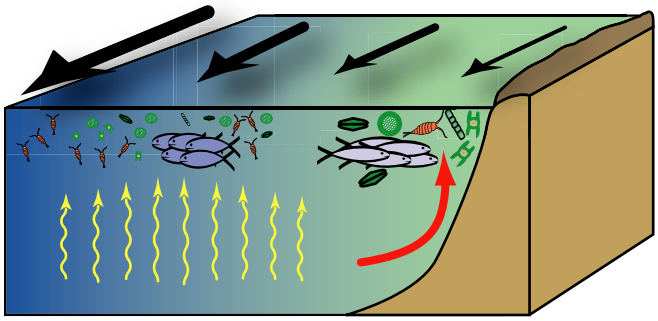

Fig. 1. Conceptual diagram displaying the hypothesized relationship between wind-forced upwelling and the pelagic ecosystem. Alongshore, equatorward wind stress results in coastal upwelling (red arrow), supporting production of large phytoplankters and zooplankters. Between the coast and the wind-stress maximum, cyclonic wind-stress curl results in curl-driven upwelling (yellow arrows) and production of smaller plankters. Anchovy (gray fish symbols) prey on large plankters, whereas sardine (blue fish symbols) specialize on small plankters. Black arrows represent winds at the ocean surface, and their widths are representative of wind magnitude.

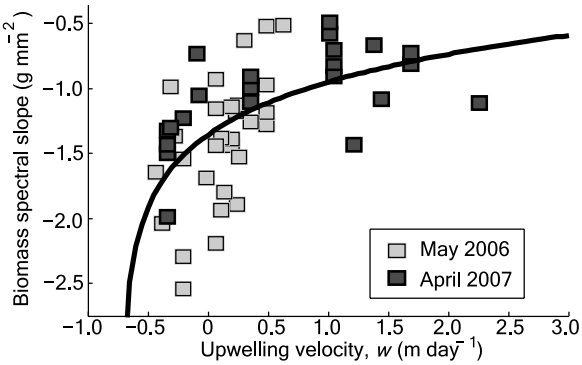

Fig. 2. Relationship between zooplankter size and upwelling rate. This relationship is modeled by using a logarithmic function ($r^2 = 0.32$, $P < 0.001$, $n = 51$, $y = 0.46 \cdot \ln(x + 0.71) - 1.20$). The mean 90% confidence interval around the slopes of the linear least-squares fits to the biomass spectra is ±0.71 g mm^{-2}.

pressure systems over the North Pacific and southwest United States (16, 17). Because these areas of positive curl are large compared with the coastal boundary region, the volume of water upwelled by slow, curl-driven upwelling is greater than that upwelled by coastal upwelling or by fast, curl-driven upwelling near the coast (15). The intensity of offshore, curl-driven upwelling is hypothesized to be related to the location of the large-scale pressure systems with respect to the coastline of California (17).

We expect the type of biological production resulting from coastal and curl-driven upwelling to differ, with high w resulting in larger phytoplankters and low w favoring smaller phytoplankters. The demand for nutrients by a phytoplankton cell is typically a function of cell volume, whereas the maximal uptake rate is a function of the cell's surface area. For this reason, smaller cells, with higher surface-area-to-volume ratios, have a competitive advantage in nutrient-limited environments (18, 19). The increased nutrient concentrations in vigorously upwelling waters (high w) reduces nutrient limitation and the competitive advantage of small cells, allowing populations of large cells with lower surface area-to-volume ratios to develop. Given that prey size correlates positively with predator size (20), larger zooplankters are favored in areas with larger phytoplankters and higher w (Fig. 1).

Temporal variability in coastal and curl-driven upwelling may affect populations of planktivorous predators by influencing production of small and large plankters. Pacific sardine spawn in offshore waters, away from areas of coastal upwelling (21), and adult and juvenile sardine have a fine mesh of gill rakers with specialized denticles to retain planktonic prey as small as 10 μm in diameter (22). Even as larvae, sardine appear to specialize on small plankters and are prevented from capturing larger prey by a small mouth-gape diameter (22, 23). In comparison, anchovy spawn near the coast (21) and use coarse gill rakers to capture larger prey (22). We hypothesize that changes in sardine population growth are related to the production of small plankters and the magnitude of curl-driven upwelling in the CCE. To test this hypothesis, we posed the following questions: Is zooplankter size related to upwelling rate? Have winds favoring curl-driven and coastal upwelling changed over decades and, if so, have these changes influenced hydrography, nutrient supply, and biological production? We examined zooplankter sizes across a gradient of upwelling rates and compared estimates of historical upwelling with concurrent measurements of water-column density, nutricline depth, chlorophyll concentration, and sardine production.

Results and Discussion

Plankter Sizes and Upwelling. A combination of data from the SeaWinds Scatterometer and shipboard and moored anemometers were used to compare w resulting from upwelling with the size of zooplankters. Zooplankton was collected during two cruises in May 2006 and April 2007 at locations spanning the CCE west of Point Conception, CA [supporting information (SI) Fig. 6]. A normalized biomass spectrum was estimated for the zooplankton collected at each station (24). The slope of the spectrum increased as w increased (Fig. 2), indicating that zooplankters are relatively larger in areas of coastal upwelling (high w) and smaller in areas of curl-driven upwelling (low w). A similar result has been found for phytoplankton in the CCE; larger phytoplankters are found nearshore where the nutricline is shallow, and smaller phytoplankters are dominant where the nutricline is deep (25).

Historic Upwelling Rates. To examine the temporal variability in coastal and curl-driven upwelling rates over the past 60 years, we used monthly averages of historic winds to calculate w of curl-driven and coastal upwelling. The geographic range of the analysis was limited to the waters off the southern and central California coasts (from Ensenada, Baja California, to Santa Cruz, CA), extending ≈300 km offshore and encompassing the area of sardine spawning off of California (SI Fig. 6). We found that regions of intense cyclonic curl are common during summer in the lee of prominent headlands and result in small areas of high w (3–7 m day^{-1}). High rates of coastal upwelling were also present at these headlands (w of 7–12 m day^{-1}). Further offshore, large regions of positive wind-stress curl and low w (0–1 m day^{-1}) were typical (Fig. 3). These results are consistent with previous studies that have examined coastal and curl-driven upwelling over smaller temporal and spatial scales (11, 26).

Although average w resulting from coastal upwelling is approximately an order of magnitude larger than w resulting from open-ocean, curl-driven upwelling, curl is more important to total upwelling transport because it covers a spatial area 18–22 times larger than the area of coastal upwelling. In our analysis, we found that wind-stress curl has been responsible for at least 60% (and up to 80%) of the annual, wind-forced upwelling transport in the southern CCE. Monthly time series of the two upwelling processes are significantly correlated ($P < 0.001$) and indicate that both coastal and curl-driven upwelling have increased since 1948. However, there are important distinctions

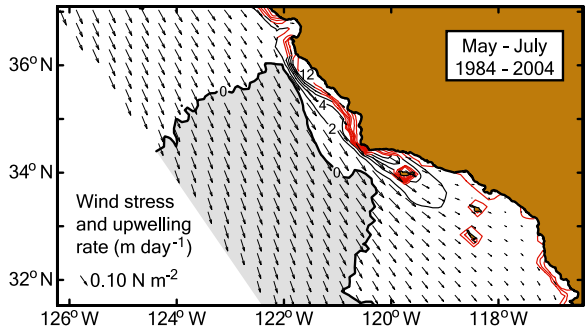

Fig. 3. Mean summertime (May–July) wind stress and upwelling rate from 1984 to 2004. Arrows indicate wind stress. Upwelling rates are denoted by contours at an interval of 2 m day^{-1}. Black contours indicate the region of curl-driven upwelling. Red contours denote coastal upwelling. Areas of anticyclonic curl (downwelling) are shaded. The years 1984–2004 correspond to the period during which nutrient, chlorophyll, and sardine production data were regularly collected.

between the two records. Vertical transport by curl-driven upwelling abruptly increased during the winters of 1975 and 1976, and the level of curl-driven upwelling remained elevated through 2004. In contrast, the coastal upwelling record shows a smaller range of variation and no abrupt changes. Coastal upwelling declined after peaking in the early 1980s. SI Fig. 7 compares w during two decades, 1950–1959 and 1990–1999.

Effects on Water Column Properties. The California Cooperative Oceanic Fisheries Investigations (CalCOFI) program has conducted quarterly surveys of temperature, salinity, chlorophyll *a* (chl *a*), and nutrients in the CCE since 1984. We compared the variability of these water-column properties to changes in upwelling during summertime cruises. We chose to focus on summer because this season corresponds to the late-larval and juvenile periods for spring-spawning sardine, and survival through these life stages is thought to be a major determinant of stock recruitment (27). Also, by focusing on summer, we avoided the issue of inconsistent timing of the spring transition with respect to the springtime CalCOFI survey.

Nutricline depth and chl *a* concentration at 10 m showed significant correlation with curl-driven upwelling from 1984 to 2004 (Fig. 4). The nutricline depth shoaled, and the chl *a* concentration increased with increases in curl-driven upwelling. The correlations between these water-column properties and

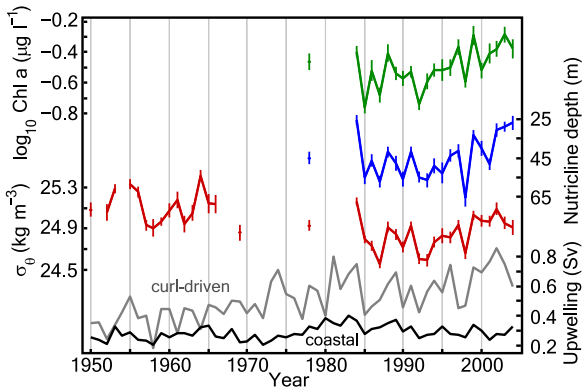

Fig. 4. Summertime upwelling, σ_θ (red line), nutricline depth (blue line), and chl *a* concentration (green line). These properties of the water column are more highly correlated with curl-driven upwelling (gray line) than with coastal upwelling (black line) after 1970. Before 1970, σ_θ is correlated with coastal upwelling and not curl-driven upwelling. (1 Sverdrup = 1×10^6 m^3 s^{-1})

Table 1. Pearson correlation coefficients between upwelling and water-column properties

Paramater	Period of comparison (no. of surveys)	Coastal upwelling	Curl-driven upwelling
Density (σ_θ)	1950–1969 (16)	**0.62, 0.67**	−0.030, 0.034
	1978–2004 (22)	0.34, **0.51**	**0.71, 0.69**
Nutricline depth	1978–2004 (22)	−0.37, **−0.60**	**−0.67, −0.62**
Log chl *a*	1978–2004 (22)	0.23, 0.57	**0.67, 0.59**

Shown are correlation coefficients (r values) between time series before and after removal of the linear trend from each time series (first and second value in each column, respectively). Bold values are significant at the 95% level.

coastal upwelling became significant only when the linear trend was removed from each time series (Table 1). We emphasize that the trend should be considered because decadal-scale variability is known to be important. The change in correlation after removing the trend indicates that consideration of decadal-scale changes in the CCE is essential to distinguish the effects of coastal and curl-driven upwelling.

We estimated potential density (σ_θ) of the upper water column using CalCOFI measurements of temperature and salinity from 1950 to the present. Surveys with reduced spatial or depth coverage (<70% of the currently sampled area) were excluded from our analysis. There were two periods of sufficient sampling: 1950–1969 (16 summers) and 1978–2004 (22 summers). Our analysis indicates that the CCE has changed over the past six decades from a system where coastal upwelling is a major factor influencing σ_θ to a system where curl-driven upwelling controls σ_θ variability (Fig. 4). Curl-driven upwelling is correlated with σ_θ only during the recent time period. In contrast, coastal upwelling is significantly correlated with σ_θ during the 1950s and 1960s (Table 1). These results are consistent with the observed increase in the contribution of wind-stress curl to the total amount of wind-forced upwelling since the 1950s.

A long-term decrease in density of the upper layers of the CCE is evident despite the increase in the total amount of wind-driven upwelling (Fig. 4). This result is in conflict with our hypothesis relating increasing wind-driven upwelling with increasing density. Our analysis of historic winds cannot account for the decrease in density between the 1960s and 1980s, suggesting that other factors, in addition to winds, have influenced σ_θ over multidecadal time periods. Vertical heat flux into the surface layers of the CCE and lateral advection of warmer waters from the south increased sharply in the mid-1970s and may be responsible for the observed decline in σ_θ (28, 29). Poleward transport in the CCE is related to positive wind-stress curl by Sverdrup balance (10, 30). Increasing levels of wind-stress curl may be associated with the poleward flux of warm waters and partially explain the differences in the relationship between σ_θ and upwelling at interannual and multidecadal scales.

Effects on Sardine Production. We compared coastal and curl-driven upwelling with surplus production per unit biomass in the sardine population over the past 22 years during which consistent stock-assessment methods have been in use. Curl-driven upwelling during late spring and summer (May–July) was positively correlated with surplus production per unit biomass. Sardine production and coastal upwelling were not correlated during these months (Fig. 5). In addition, we examined the influence of coastal and curl-driven upwelling on surplus production per unit biomass by using a stepwise regression model. The model, which included curl-driven upwelling during May–July explained a significant portion of the variance in production. Addition of coastal upwelling did not significantly improve model fit ($P >$

ECOLOGY

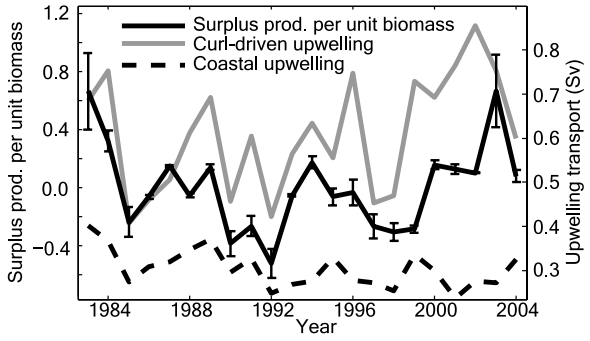

Fig. 5. Upwelling and surplus production per unit biomass of Pacific sardine. Curl-driven upwelling from May through July showed the highest correlation with surplus production per unit biomass ($r = 0.62$, $P < 0.005$, $n = 22$). Coastal upwelling during the same period was not significantly correlated with production ($r = 0.40$, $P = 0.067$, $n = 22$). Error bars are ± one standard deviation of the sardine production estimates.

0.05). Curl-driven and coastal upwelling records were not correlated over this time period (Fig. 5).

In addition, we compared the influence of coastal upwelling, curl-driven upwelling, and sea-surface temperature (SST) on sardine production using environmentally dependent surplus production (EDSP) models during two periods for which environmental and fisheries data are available: 1948–1962 and 1983–2004. SST has been shown to be reasonably effective in explaining the dynamics of sardine biomass in EDSP models (31), and we were interested in testing whether SST or a measure of upwelling produced the best estimate of sardine production. We found that use of curl-driven upwelling in the model produced the best fit to observed production during both periods (SI Fig. 8). The model using SST as the environmental variable was more successful than that using coastal upwelling, and all three environmental variables performed better than the null model (which did not include environmental variability). The sum of squared deviations for the model using curl-driven upwelling was 0.30 MT^2. Values for the models using SST and coastal upwelling were 0.44 MT^2 and 0.47 MT^2, respectively. The null model resulted in a sum of squared deviations equal to 0.51 MT^2.

Although use of curl-driven upwelling in the EDSP models produced the best estimates of sardine production during both time periods, the months during which curl produced the best estimate shifted between 1948–1962 and 1983–2004. In the more recent period, use of curl-driven upwelling during May–July was optimal for estimating production and suggests that conditions during these months were most influential in determining sardine production. Since 1983, extensive spawning has occurred off of central and southern California in April (32). May–July corresponds to the early life-history stages during which the environment has the strongest influence on survival (27). Use of curl-driven upwelling during October, November, and December produced the best model performance during the 1948–1962 period. This result is consistent with the observation that spawning in autumn offshore of Baja California is more important to sardine production during periods of low population size (32). The months of SST and coastal upwelling that produced the best estimates of production also shifted from late summer and autumn during the 1958–1962 period to spring and early summer during the 1983–2004 period.

Consideration of Other Upwelling Systems. The CCE is the only upwelling system with the environmental time series required to investigate wind-forced upwelling and the response of water-column properties and fisheries production at decadal and multidecadal scales. Observations of historic, oceanic winds depend on ship traffic, and the number of observations in the CCE is high compared with other eastern boundary currents (16). Atmospheric models offering high-resolution estimates of wind stress over the past 60 years have not yet been developed in other regions of the globe. In addition, the long-term hydrographic datasets provided by the CalCOFI program are unique.

Wind-forced upwelling results in high primary and fisheries production in eastern boundary currents around the world (8), and the concepts presented here are applicable to each of these regions. However, the effects of coastal and curl-driven upwelling may vary with conditions specific to each area. For instance, latitudinal differences may have a significant influence on w and production of plankton and fish. The rate of curl-driven upwelling in the Humboldt Current Ecosystem (HCE) off the coast of Peru will be more than three times that in the CCE for a given wind-stress curl because of the difference in the Coriolis parameter with latitude. A wind-stress curl of $0.5 \cdot 10^{-6}$ N m^{-3} at 35° N latitude in the CCE will result in w of 0.5 m day^{-1}. The same level of cyclonic wind-stress curl at 10° S latitude in the HCE will create w of 1.7 m day^{-1}. Much larger plankter sizes may result from curl-driven upwelling in the HCE. Anchovy feed most effectively on large plankters (22), and we would expect the HCE to be dominated by anchovy and support a larger anchovy population than the CCE under similar curl conditions. Consistent with this hypothesis, anchovy is the dominant fish species in Peru, whereas sardine is dominant in the CCE. Annual anchovy landings in Peru peaked at >13 MT in the mid 1970s, whereas maximal landings in California peaked at ≈0.4 MT in the early 1980s (1).

Our results demonstrate a mechanism, from physics to fish, relating variability in production of Pacific sardine to environmental changes over interannual and decadal scales. We show that the level of production in a large, marine ecosystem depends on wind-stress curl. Coupling predictions of atmospheric winds with a simple hydrographic model will allow forecasting of sardine production in the CCE. Such forecasts have increasing ecological and economic value as globalization of commerce and industrialization of fisheries continue in response to growing demand and utilization of marine resources (33). Simultaneously, predictions of future climate conditions are becoming more precise (34) and offer an opportunity to more effectively manage fisheries if the biological responses to physical variability are understood. Credible mechanistic hypotheses relating atmospheric physics to variability in the ocean's biota are essential to prudently manage marine resources under a changing climate.

Materials and Methods

May 2006 and April 2007 Cruise Data. Zooplankton samples were collected during research cruises in May 2006 and June 2007 as part of the CCE Long-Term Ecological Research program. Cruises were structured to sample across the CCE, ranging from areas of coastal upwelling to offshore, oligotrophic areas. Zooplankton was sampled by using a BONGO net of 202-μm-Nitex mesh, towed obliquely to 210 m (depth permitting) between 2100 and 0400 hours following the strict protocol of the CalCOFI program (35). Three-eighths of the sample from one BONGO codend was wet-sieved through nested screens of 5,000, 2,000, 1,000, 505, and 202 μm, and dry masses in each size class were determined (36). A linear least-squares line was fit to approximate the biomass-size spectrum for each sample according to the following formula:

$$\log \frac{B_x}{\Delta x} = m[\log(x)] + b,$$

where B_x is the sample biomass retained on a filter of mesh size x, Δx is the size interval for each fraction (taken here as 5,000, 3,000, 1,000, 495, and 303 μm), and m and b are the slope and y-intercept of the linear, best-fit line.

Wind-stress data collected by the SeaWinds Scatterometer were used to estimate w. For two sampling stations near the coast where scatterometer

data are invalid, wind stresses were estimated by using data from the shipboard anemometer and moored buoys operated by the National Data Buoy Center. A standard algorithm was used to convert wind speed to wind stress (37). Coastal and curl-driven upwelling rates were calculated as described below and averaged over 5 days before zooplankton collection.

Historic Upwelling Estimates. We used output from a dynamically downscaled model of historic winds (1948–2005) from the National Centers for Environmental Prediction and National Center for Atmospheric Research (NCEP/NCAR) Reanalysis. This model, known as CaRD10 (California Reanalysis Downscaling at 10 km) produces fine-scale, thermodynamically consistent atmospheric variables without deviation from the original NCEP/NCAR reanalysis data (38). CaRD10 was chosen for use in this analysis because it is the only atmospheric model offering the ability to examine mesoscale variability in curl-driven upwelling at multidecadal scales. The CaRD10 model covers a large spatial area and offers a historical perspective unparalleled by models of similar resolution. Compared with observed wind speed, the CaRD10 model shows significant improvement over other models that offer a historical perspective at lower resolution. This improvement is especially evident in the coastal ocean (38). We recognize that wind stress at the coast is difficult to model, even with grids of higher resolution. However, we feel that the CaRD10 model provides the best available data on the spatial and temporal scales relevant to the sardine habitat in the southern CCE.

Upwelling transport is defined as the upward movement of a volume of water per unit time and results from two different processes: curl-driven upwelling or coastal upwelling. We used monthly averages of surface wind stress (N m^{-2}) produced by the CaRD10 model to calculate the vertical velocity, w_{curl} (m s^{-1} positive upward), of curl-driven upwelling at the base of the mixed layer (39):

$$w_{\mathrm{curl}} = \frac{1}{\rho_{\mathrm{w}} f} \nabla \times \tau,$$

where $\nabla \times \tau$ is the curl of the wind-stress field, ρ_w is seawater density (taken as 1,024 kg m^{-3}), and f is the Coriolis parameter. Wind-stress derivatives used in the calculation of curl at a given grid point were taken as the difference between wind stresses at adjacent grid points.

Coastal upwelling due to seaward Ekman transport was also calculated by using output from the CaRD10 model. T, the volume of Ekman transport per meter of coastline (m^3 s^{-1} per meter of coast), was estimated (39):

$$T = \frac{\tau_a}{\rho_w f},$$

where τ_a is alongshore wind stress within 10 km of the coastline. Conservation of mass requires that volume transport by coastal upwelling be equivalent to T. This volume transport was divided by the local Rossby radius of deformation, R_d, to yield a mean vertical velocity of coastal upwelling, w_{coast} (m s^{-1}):

$$w_{\mathrm{coast}} = \frac{T}{R_d}.$$

Based on earlier studies in the region, a Rossby radius of 10 km was used in the calculation (11, 13). Upwelling by each mechanism was integrated over the spatial domain to generate indices of upwelling transport by coastal and curl-driven upwelling. The relative magnitudes of coastal and curl-driven upwelling are subject to the R_d used as the location of the boundary between coastal and curl-driven upwelling processes. However, variation in the two time series is not influenced by changes in the boundary location.

Historic Hydrographic, Chemical, and Biological Measurements. Temperature, salinity, and concentrations of nitrate and chl *a* have been regularly measured by the CalCOFI program since 1984 (40). We defined the nutricline depth as the first depth at which nitrate concentration exceeded 1.0 μmol l^{-1}. Chl *a* concentration was that measured at 10 m. CalCOFI measurements of temperature, salinity, and pressure at 50 m were used to estimate σ_θ (41). These measures of nutricline depth, chl *a*, and σ_θ were averaged over the standard CalCOFI sampling grid (i.e., lines 76.7 to 93.3 and from station 90.0 to the coast) to yield a mean value for each cruise. Historic upwelling transport was averaged from June–August for comparison with density, nutricline depth, and chl *a* concentration. This period encompasses the range of summertime CalCOFI sampling (except for 1985 and 1986, when CalCOFI cruises occurred in September). Temperature and salinity at 50 m were sampled by the CalCOFI surveys before 1983.

Historic SST. The SST data were from the Comprehensive Oceanographic–Atmospheric Data Set (42) and covered the spatial domain used in the upwelling estimation. Resolutions of the data were 1° × 1° from 1960 to the present and 2° × 2° from 1948 to 1959.

Pacific Sardine Production. Stock assessments have been performed for sardine since 1982 by using an age-structured population model incorporating both fishery-dependent and fishery-independent data (U.S. Department of Commerce, Technical Memorandum NOAA-TM-NMFS-SWFSC-396). By using these data, annual surplus production (ASP) was calculated for the sardine stock from 1983 to 2004. ASP is as a measure of annual growth in the total biomass of the stock and is largely a function of the recruitment of young fish. ASP in year t is approximated as

$$ASP_{\mathrm{t}} = (b_{0,t} + \delta C_{0,t}) + (b_{1+,t} - b_{1+,t-1} + \delta C_{1+,t}),$$

where $b_{a,t}$ and $C_{a,t}$ are the biomass and catch of age a fish at time t (age 0 fish are those between 0 and 1 year old; age 1+ fish are those older than 1 year), and δ is a catch adjustment factor (0.83) as estimated empirically for the California stock of Pacific sardine (31). The catch adjustment factor converts the catch during the preceding fishing season to its biomass estimated at the end of the fishing season had the fish remained in the population. This accounts for the portion (δ) of captured fish that would have survived to the end of the fishing season had they not been harvested. Surplus production per unit biomass was calculated by dividing ASP by the biomass of sardine at ages 1+. The time series of surplus production per unit biomass showed a declining trend as the sardine biomass expanded in the 1980s and 1990s. This trend is likely a result of the decrease in recruitment per spawner that is characteristic of an increasing fish population (density-dependent recruitment) and is independent of environmental variability (43). This linear trend in the time series was removed before comparison with upwelling estimates to prevent correlation based solely on the long-term trend resulting from density-dependent changes in recruitment.

We limited our calculation of surplus production per unit biomass to the period since 1983, when the stock assessment methods have been consistent and incorporated both fishery-independent and -dependent data. No stock assessment for sardine was conducted from 1963 to 1981. The stock assessments performed before 1963 were based on fishery-dependent data (44). We used previously calculated estimates of ASP for the sardine stock from 1948 to 1962 (31).

Population Modeling. We modified the Fox surplus production model so that the carrying capacity of the population varies annually as a function of environmental conditions (45). The conventional Fox model estimates ASP in year t as follows:

$$ASP_t = rB_{\mathrm{t}} \left(1 - \frac{\ln[B_t]}{\ln[K]}\right),$$

where r is the intrinsic rate of increase, B_t is the stock biomass (ages 1+), and K is a constant equal to B_{max}, the population carrying capacity. To construct an EDSP model, an environmentally dependent variable (related to upwelling or SST) was included in the equation such that the carrying capacity K was a function of the environmental condition in year t as well as the population carrying capacity, B_{max}:

$$K = B_{\max}(E_t + \alpha),$$

where E_t is an index of environmental condition and α is a constant scaling parameter. Parameters r, B_{max}, and α (each greater than zero) are estimated during the model fitting procedure. This model structure assumes that the environmental variables are positively related to ASP in the sardine population.

Because survival through larval and early juvenile life stages is thought to be a major determinant of stock recruitment (27), sardine production is likely affected more by environmental conditions in the first months after the hatching of larvae than by conditions throughout the entire year. Instead of comparing annual fish production with upwelling estimates averaged over a 12-month period, estimates from each period of three consecutive months were averaged to generate annual time series of conditions specific to each 3-month period. Each time series was standardized by subtracting the minimum value and dividing by the standard deviation. The resulting standardized time series was included in the EDSP model as E_t. Model parameters and

performance were determined by minimizing the sum of squared deviations between the modeled and observed ASP.

In the stepwise regression procedure, the environmental time series explaining most of the variability in surplus production per unit biomass was included in as the first explanatory time series in the model. Additional environmental time series were included only if inclusion significantly improved model fit ($P < 0.05$).

ACKNOWLEDGMENTS. We are grateful to M. Kanamitsu for development of the atmospheric model and thank P. Franks, M. Landry, D. Rudnick, M. Ohman, three anonymous reviewers, and R.E.D., the communicating member, for their comments. The 2006 and 2007 cruises were supported by the CCE Long-Term Ecological Research Program, and the CalCOFI program provided historical data. This work was supported by the National Science Foundation Graduate Research Fellowship Program, the Michael M. Mullin Fund, and the Maxwell–Fenmore Fellowship.

1. Lluch-Belda D, *et al.* (1989) Worldwide fluctuations of sardine and anchovy stocks: The regime problem. *S Afr J Mar Sci* 8:195–205.
2. Cury P, *et al.* (2000) Small pelagics in upwelling systems: Patterns of interaction and structural changes in ''wasp-waist'' ecosystems. *ICES J Mar Sci* 57:603–618.
3. Baumgartner TR, Soutar A, Ferreirabartrina V (1992) Reconstruction of the history of Pacific sardine and northern anchovy populations over the past 2 millennia from sediments of the Santa-Barbara Basin, California. *CalCOFI Rep* 33:24–40.
4. Hsieh CH, *et al.* (2006) Fishing elevates variability in the abundance of exploited species. *Nature* 443:859–862.
5. Chavez FP, Ryan J, Lluch-Cota SE, Niquen M (2003) From anchovies to sardines and back: Multidecadal change in the Pacific Ocean. *Science* 299:217–221.
6. Peterson WT, Schwing FB (2003) A new climate regime in Northeast Pacific ecosystems. *Geophys Res Lett* 30, 10.1029/2003GL017528.
7. Bakun A, Broad K (2003) Environmental ''loopholes'' and fish population dynamics: comparative pattern recognition with focus on El Nino effects in the Pacific. *Fish Oceanogr* 12:458–473.
8. Ryther JH (1969) Photosynthesis and fish production in sea. *Science* 166:72–76.
9. Yoshida K, Mao HL (1957) A theory of upwelling of large horizontal extent. *J Mar Res* 16:40–54.
10. Chelton DB (1982) Large-scale response of the California Current to forcing by the wind stress curl. *CalCOFI Rep* 23:30–148.
11. Pickett MH, Paduan JD (2003) Ekman transport and pumping in the California Current based on the U.S. Navy's high-resolution atmospheric model (COAMPS). *J Geophys Res* 108:332.
12. Chelton DB, Schlax MG, Freilich MH, Milliff RF (2004) Satellite measurements reveal persistent small-scale features in ocean winds. *Science* 303:978–983.
13. Pickett MH, Schwing FB (2006) Evaluating upwelling estimates off the west coasts of North and South America. *Fish Oceanogr* 15:256–269.
14. Di Lorenzo E (2003) Seasonal dynamics of the surface circulation in the Southern California Current System. *Deep-Sea Res Part II Top Stud Oceanogr* 50:2371–2388.
15. Dever EP, Dorman CE, Largier JL (2006) Surface boundary-layer variability off Northern California USA, during upwelling. *Deep-Sea Res Part II Top Stud Oceanogr* 53:2887–2905.
16. Bakun A, Nelson CS (1991) The seasonal cycle of wind-stress curl in subtropical eastern boundary current regions. *J Phys Oceanogr* 21:1815–1834.
17. Edwards KA, Rogerson AM, Winant CD, Rogers DP (2001) Adjustment of the marine atmospheric boundary layer to a coastal cape. *J Atmos Sci* 58:1511–1528.
18. Margalef R (1978) Life-forms of phytoplankton as survival alternatives in an unstable environment. *Oceanol Acta* 1:493–509.
19. Falkowski PG, Oliver MJ (2007) Mix and match: How climate selects phytoplankton. *Nat Rev Microbiol* 5:813–819.
20. Moloney CL, Field JG (1991) The size-based dynamics of plankton food webs. 1. A simulation-model of carbon and nitrogen flows. *J Plank Res* 13:1003–1038.
21. Checkley DM, Jr, Dotson RC, Griffith DA (2000) Continuous, underway sampling of eggs of Pacific sardine (*Sardinops sagax*) and northern anchovy (*Engraulis mordax*) in spring 1996 and 1997 off Southern and Central California. *Can J Fish Aquat Sci* 47:1139–1155.
22. van der Lingen CD, Hutchings L, Field JG (2006) Comparative trophodynamics of anchovy *Engraulis encrasicolus* and sardine *Sardinops sagax* in the southern Benguela: are species alternations between small pelagic fish trophodynamically mediated? *Afr J Mar Sci* 28:465–477.
23. Arthur DK (1976) Food and feeding of larvae of three fishes occurring in the California Current, *Sardinops sagax*, *Engraulis mordax*, and *Trachurus symmetricus. Fish Bull* 74:517–530.
24. Platt T, Denman K (1978) The structure of pelagic marine ecosystems. *Rapp P-V Réun Cons Int Explor Mer* 173:60–65.
25. Mullin MM (1998) Biomasses of large-celled phytoplankton and their relation to the nitricline and grazing in the California Current System off Southern California, 1994–1996. *CalCOFI Rep* 39:117–123.
26. Koracin D, Dorman CE, Dever EP (2004) Coastal perturbations of marine-layer winds, wind stress, and wind stress curl along California and Baja California in June 1999. *J Phys Oceanogr* 34:1152–1173.
27. Jennings S, Kaiser MJ, Reynolds JD (2001) *Marine Fisheries Ecology* (Blackwell Science, Oxford), pp 78–83.
28. Miller AJ, Cayan DR, Barnett TP, Graham NE, Oberhuber JM (1994) Interdecadal variability of the Pacific Ocean - Model response to observed heat flux and wind stress anomalies. *Clim Dyn* 9:287–302.
29. Di Lorenzo E, Miller AJ, Schneider N, McWilliams JC (2005) The warming of the California Current System: Dynamics and ecosystem implications. *J Phys Oceanogr* 35:336–362.
30. Munk WH (1950) On the wind-driven ocean circulation. *J Met* 7:79–93.
31. Jacobson LD, Bograd SJ, Parrish RH, Mendelssohn R, Schwing FB (2005) An ecosystem-based hypothesis for climatic effects on surplus production in California sardine (*Sardinops sagax*) and environmentally dependent surplus production models. *Can J Fish Aquat Sci* 62:1782–1796.
32. Smith PE (2005) A history of proposals for subpopulation structure in the Pacific sardine (*Sardinops sagax*) population off western North America. *CalCOFI Rep* 46:75–82.
33. Pauly D, Watson R, Alder J (2005) Global trends in world fisheries: Impacts on marine ecosystems and food security. *Phil Trans R Soc London Ser B* 360:5–12.
34. Barnston AG, Kumar A, Goddard L, Hoerling MP (2005) Improving seasonal prediction practices through attribution of climate variability. *Bull Am Met Soc* 86:59–72.
35. Ohman MD, Smith PE (1995) A comparison of zooplankton sampling methods in the CalCOFI time series. *CalCOFI Rep* 36:153–158.
36. Harris R, Wiebe P, Lenz J, Skjoldal HR, Huntley M (2000) *ICES Zooplankton Methodology Manual* (Academic, San Diego), pp 90–94.
37. Yelland MJ, M*et al.* (1998) Wind stress measurements from the open ocean corrected for airflow distortion by the ship. *J Phys Oceanogr* 28:1511–1526.
38. Kanamitsu M, Kanamaru H. (2007) 57-year California reanalysis downscaling at 10 km (CaRD10). Part I: System detail and validation with observations. *J Clim* 20:5553–5571.
39. Smith RL (1968) Upwelling. *Oceanogr Mar Biol Ann Rev* 6:11–46.
40. Hayward TL (2000) El Nino 1997–98 in the coastal waters of Southern California: A timeline of events. *CalCOFI Rep* 41:98–116.
41. Gill AE (1982) *Atmosphere–Ocean Dynamics* (Academic, New York), pp 326–408.
42. Woodruff SD, Slutz RJ, Jenne RL, Steurer PM (1987) A comprehensive ocean-atmosphere data set. *Bull Am Met Soc* 68:1239–1250.
43. Beverton RJH, Holt SJ (1957) *On the Dynamics of Exploited Fish Populations* (Chapman and Hall, London), pp 44–65.
44. MacCall AD (1979) Population estimates for the waning years of the Pacific Sardine fishery. *CalCOFI Rep* 20:79–82.
45. Fox WW (1970) An exponential surplus-yield model for optimizing exploited fish populations. *Trans Am Fish Soc* 99:80–88.